CALIBRATION OF THE BIG BEAR VIDEOMAGNETOGRAPH

JOHN R. VARSIK
Big Bear Solar Observatory, California Institute of Technology, Pasadena, CA 91125, U.S.A.

(Received 4 February, 1994; in revised form 18 April, 1995)

Abstract. The Big Bear videomagnetograph is calibrated using three methods. Longitudinal magnetograms are calibrated by using the differences in radial velocity of the Sun caused by solar rotation, or by measuring the line profile in the Zeeman-sensitive 6103 Å line used by the magnetograph system. Transverse magnetograms can be calibrated by obtaining spectra in the more magnetically sensitive 5250 Å line which measure the total magnetic field and then subtracting the longitudinal component. The calibration of the transverse magnetograms is in agreement with that obtained by line profile measurements. Observations of an active region on 1993 March 8 with both the magnetograph system and with the BBSO spectrograph showed that good agreement was found between all three methods, provided the effect of seeing on the magnetograms is allowed for. Magnetograph saturation does not occur for magnetic fields below about 2100 G.

1. Introduction

This subject was previously discussed by Shi, Wang, and Patterson (1986). I have revised the discussion here to reflect the current videomagnetograph instrument and its operation. The calibrations described here permit quantitative measurements to be made with the videomagnetograph system.

All magnetographs measure solar magnetic fields by using the Zeeman effect. The Zeeman splitting produced by the solar magnetic fields is

$$\Delta\lambda_H = 4.67 \times 10^{-13}\lambda^2 g H \,, \tag{1}$$

wavelength in ångstroms, magnetic field in gauss. For fields along the line of sight, a single absorption line is split into two components with opposite circular polarizations. For magnetic fields at 90° to the line of sight, three components are formed, one at the original wavelength but with linear polarization parallel to the direction of the magnetic field, and two offset by the splitting given above with linear polarization perpendicular to the magnetic field. The first photoelectric magnetograph was operated by Babcock and Babcock (1952).

The videomagnetograph evolved from Leighton's (1959) original photographic subtraction technique, which replaced the spectroheliograph used by Babcock with a narrow-band tunable filter. As in the Babcock instrument, the relative wavelength shift between the right and left circular polarized Zeeman components caused a difference in intensity, which in Leighton's instrument was detected by superposing a photographic negative of one polarity on a positive of the other polarity and making a print of the result. The circular analyzer for the videomagnetograph

Solar Physics **161:** 207–228, 1995.

is made up of a potassium dihydrogen phosphate Pockels cell (KDP) used as a $\pm\frac{1}{4}$-wave plate and the polarizer in the first element of a birefringent filter. The fast axis of the KDP is oriented so that it is at $\pm 45°$ to the filter's polarization axis when voltage is applied.

The original Big Bear videomagnetograph (VMG) was built by Smithson and Leighton (Smithson and Leighton, 1971; Smithson, 1972). A detailed discussion of the original VMG system can be found in Mosher (1976). In this instrument video signals were stored and subtracted using an analog video disk, rather than the tedious photographic process. The final magnetogram produced was recorded by photographing the video display with a 35 mm camera. Results were limited by the high noise levels built up by repeated recording of the video signals during the integration process.

The first digital system using the Quantex image processor and a PDP11 computer was built in 1979 (Zirin, 1986). In this system video frames were acquired by the digital image processor directly from the camera, thus eliminating the noise generated by the analog video disk. The resulting digital magnetograms were saved to disk and/or tape as well as photographed. Dynamic range of the instrument was limited by the expense of computer memory at the time, and the speed and addressing limitations of the PDP11 computer system limited the amount of pipeline processing that could be done on a data set. Calibration of this system was discussed by Shi, Wang, and Patterson (1986).

In order to be able to observe simultaneously in two lines, a second magnetograph system was considered desirable. A new Datacube image processor and VAX computer was purchased at the end of 1988, and a magnetograph system with the same capabilities as the original Quantex image processor/PDP11 system was operating by the end of 1989.

At that time it was considered useful to increase the dynamic range of the magnetograph output images from the 8-bit slice (out of a 12-bit buffer) that the Quantex/PDP11 system was capable of to full 16-bit capability. It was also determined that real-time division by intensity was desirable for active region magnetic field measurements. Additional memory for the Datacube processor was obtained and new software was written with these capabilities by early 1991. Developments have continued since then to improve the speed of operation and add additional features.

Improvements to the VMG system other than changes in the image processing system since the Shi, Wang, and Patterson (1986) paper include:

(1) Replacement of the RCA Newvicon camera with a Cohu model 4812 solid-state camera. The Cohu camera, which uses a CCD detector, is much more linear, stable, and sensitive than the older tube-type cameras. The Cohu camera is now operated with fixed black level and fixed amplifier gain. This greatly simplifies the process of locating the true zero-intensity signal level. The solid-state camera also eliminates the need for 'dead time' between KDP orientations and makes

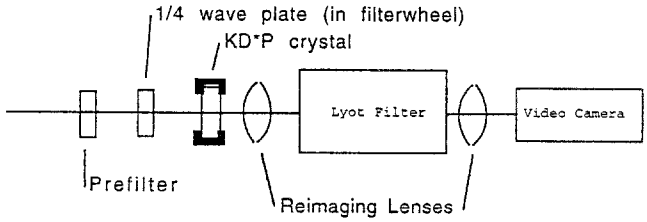

Fig. 1. Schematic diagram of the Big Bear videomagnetograph system set up for 6103 Å. The $\frac{1}{4}$-wave plates (one for Q, one for U, at orientations 45° apart) in the filterwheel are only used for transverse field measurements, and are replaced by a circular polarizer for velocity images and an empty position for longitudinal magnetograms. The KDP fast axes are at ±45° from the axis of the polarizer in the first element of the Zeiss filter.

integrations roughly twice as fast as the older system for the same number of video frames.

(2) Replacement of the original mica $\frac{1}{4}$-wave plate (used in double bandpass mode) by an achromatic retarder.

(3) Enclosure of the KDP crystal together with the Zeiss filter in a foam-core cabinet for better temperature stability. The waste heat from the Zeiss filter also keeps the KDP crystal from freezing at night in the winter.

(4) Addition of a computer-controlled filterwheel. This is mounted between the prefilter and the KDP crystal, and holds the circular polarizer for Dopplergrams, $\frac{1}{4}$-wave plates for transverse magnetograms, and neutral-density filters to adjust the light level for longitudinal magnetograms. The $\frac{1}{4}$-wave plates are positioned with fast axes at 45° (for Q) and 90° (for U) relative to the geocentric E–W horizontal axis of the video camera. The processing capability of the VAX computer allows the production of quick-look transverse field direction maps in real time.

The Big Bear VMG system is typically used at the Ca I 6102.727 Å line. The wavelength discrimination at 6103 Å is supplied by a Zeiss tunable birefringent filter. The VMG at 6103 Å can be operated in two modes, known as single bandpass (SBP) mode and double band pass (DBP) mode (Ramsey, 1971). In single bandpass mode the instrument is generally used in the blue wing of the line. This reduces the background brightness variations caused by granulation, since the increase in brightness due to a rising granule is canceled by the blueshift of the absorption line. The magnetograph has also been used at 6439 Å, Hα (SBP mode only), and 7700 Å (using K absorption cells as filters, see Cacciani, Varsik, and Zirin, 1989). This paper discusses only the current Datacube VMG system at 6103 Å.

The optical characteristics of the Datacube system are the same as those of the Quantex system (Zirin, 1986). Figure 1 shows a schematic diagram of the optical system of the Big Bear videomagnetograph, not including the telescope. The telescope used with the magnetograph is generally the Big Bear 25-cm telescope, a straight-through refractor consisting of a vacuum tank with the primary lens serving as the front window, a relay lens on a motorized stage used to adjust the

focus, and an exit window. For measurement of longitudinal fields, after leaving the vacuum tank and passing through heat-reflecting glass and a prefilter the light passes through the KDP crystal. Because the camera is quite sensitive to infrared radiation and ordinary prefilters often do not block infrared well, an infrared-blocking filter should always be used as part of the filter train. The KDP crystal acts alternately as a $+\frac{1}{4}$-wave or $-\frac{1}{4}$-wave plate depending on the polarity of the voltage applied to it. After passing through the KDP crystal, the light enters the Zeiss birefringent filter. The filter is actually mounted backwards, so that the light passes first through the $\frac{1}{4}$ Å element. In single bandpass mode the entrance (formerly exit) polaroid is left in the beam. This (together with the KDP) acts as a circular analyzer in which the direction of circular polarization passed depends on the polarity of the voltage applied to the crystal.

In double bandpass mode the entrance polaroid is flipped out (setting the filter to $\frac{1}{2}$ Å mode in normal use). The filter is tuned so that the passband (when the KDP is not modulated) is centered on the line. A $\frac{1}{4}$-wave plate is inserted between the KDP crystal and the filter, with the fast axis oriented 45° to the axis of the filter polaroid (when it is inserted). This arrangement allows opposite linear polarizations (depending on the KDP voltage) to be transmitted through the filter simultaneously, one $\frac{1}{8}$ Å redward and one $\frac{1}{8}$ Å blueward of the nominal center of the filter passband (the combination of these two bandpasses is what increases the bandpass of the filter from $\frac{1}{4}$ to $\frac{1}{2}$ Å in normal use).

For transverse field measurements, the filter is used in single bandpass mode. A $\frac{1}{4}$-wave plate is flipped into the beam ahead of the KDP crystal by a filterwheel, thus converting linear polarized light of the desired orientation to circular polarization (and circular polarized light to linear polarization) for detection by the rest of the optical system.

For velocity measurements, the filter is used in double bandpass mode, and a circular polarizer is flipped into the beam ahead of the KDP crystal. Thus all of the light (on both sides of the line center) is converted to a single circular polarization. As the KDP is modulated, the light which is allowed to pass through the system comes alternately from one or the other side of the line center.

As the KDP is modulated, the video frames are added to or subtracted from the contents of a memory buffer (initialized to zero). Thus a difference signal is accumulated in the buffer during integration. The major differences between the Quantex and Datacube systems have to do with how the video frames are stored and processed once they are acquired. The Quantex system stores its signals as 8-bit unsigned integers. The signal corresponding to zero magnetic field is stored as the value 128, while positive magnetogram signals are stored as values greater than 128 and negative signals are stored as values less than 128. The Datacube system uses 16-bit signed integers, with the zero magnetic field signal stored as zero. The Datacube system is always operated so that black sky digitizes to a value of zero in an intensity image. This is generally not true of the Quantex system.

The Big Bear videomagnetograph is intended primarily for the purpose of making 'magnetogram movies', that is, records of the changes in active region and quiet-Sun magnetic fields with high time resolution. In order to do this in a practical way, some concessions have to be made in the accuracy of the magnetic field measurements. Therefore, the calibration methods used must be simplified and quickly applicable to the data. So, we do not attempt to measure the field in multiple spectral lines nor do we attempt to measure multiple wavelength offsets for every image we obtain. This implies that the filling factor f, the fraction of a resolution element containing magnetic field cannot be measured. This could introduce a problem in observing transverse fields in the quiet Sun, where small filling factors could be expected, since neglect of the filling factor could have the effect of overestimating the strength of the transverse field relative to the longitudinal field. In active regions f is probably close to 1, but in the quiet Sun f may be much smaller. Since the sensitivity of the current Big Bear magnetograph to transverse fields is such that we cannot reliably measure transverse fields outside of active regions at the present time, I will assume that $f = 1$ in all cases.

An example of the results possible with the BBSO magnetograph is shown in Figure 2, compared with a magnetogram produced by the NASA/NSO spectromagnetograph. Both images were obtained 6 August, 1993 and show NOAA AR 7558. The NASA/NSO image is a small portion of the daily full-disk magnetogram taken at a pixel size of about 1×1 arc sec. The size of the pixels in the BBSO instrument was 0.73×0.58 arc sec. Both instruments are capable of observing the full disk of the Sun in about 40 min.

The contour shown in Figure 2(a) surrounds a small magnetic feature at the 200 G level. The average field in the feature is 300 G, with a maximum measured field of 430 G. The flux in the feature is 7.8×10^{17} Mx.

The Big Bear magnetograph was mounted on the Big Bear 25-cm refractor, and the instrument was operated in the single bandpass mode. The final image used 64 video frames, 32 in each KDP polarity. The integration time was just over 2 s. For higher resolution work the magnetograph can also be mounted on the 65-cm Gregorian reflector. Although the figure shows an integration of 64 video frames, the instrument can integrate from 2 frames (producing $\frac{1}{15}$ s exposure time to limit the effects of seeing) up to more than 4096 frames in one observation allowing very weak fields (on the order of 10 G) to be measured. For very long integrations (longer than 4096 frames) we find that better results are obtained by reregistering and co-adding multiple 4096-frame magnetograms than are obtained with long single exposures. This is most likely due to image motion during such long integrations.

Intercomparison of an older version of the Big Bear magnetograph with the magnetographs at the Huairou Solar Observing Station of Beijing Astronomical Observatory and at the Mees Solar Observatory of the University of Hawaii (Wang *et al.*, 1992) shows that the morphology of both longitudinal and vector magne-

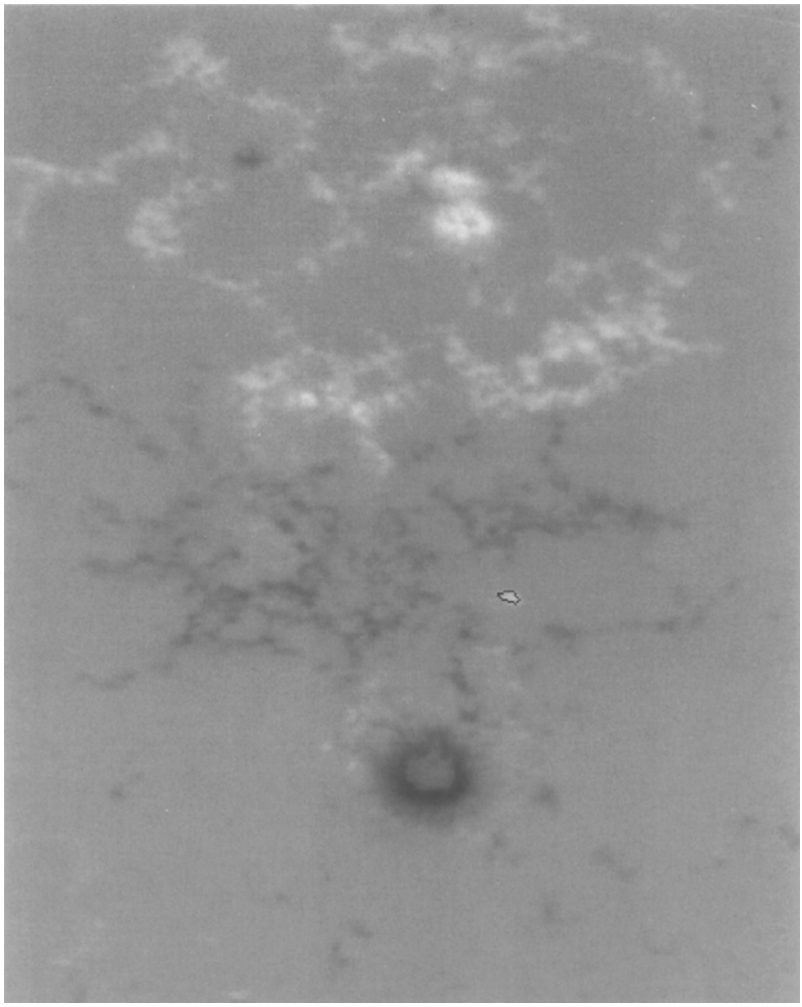

Fig. 2a.

tograms obtained at the three sites are consistent with each other. The Big Bear vector magnetograms also matched the morphology of Hα features well.

2. Calibration Methods

The VMG can be calibrated in DBP mode using the 'Doppler calibration' method (described below). This is the standard method of calibration which has been used at Big Bear Solar Observatory in the past (Shi, Wang, and Patterson, 1986). The SBP mode system can also be calibrated directly using the slope of the absorption line.

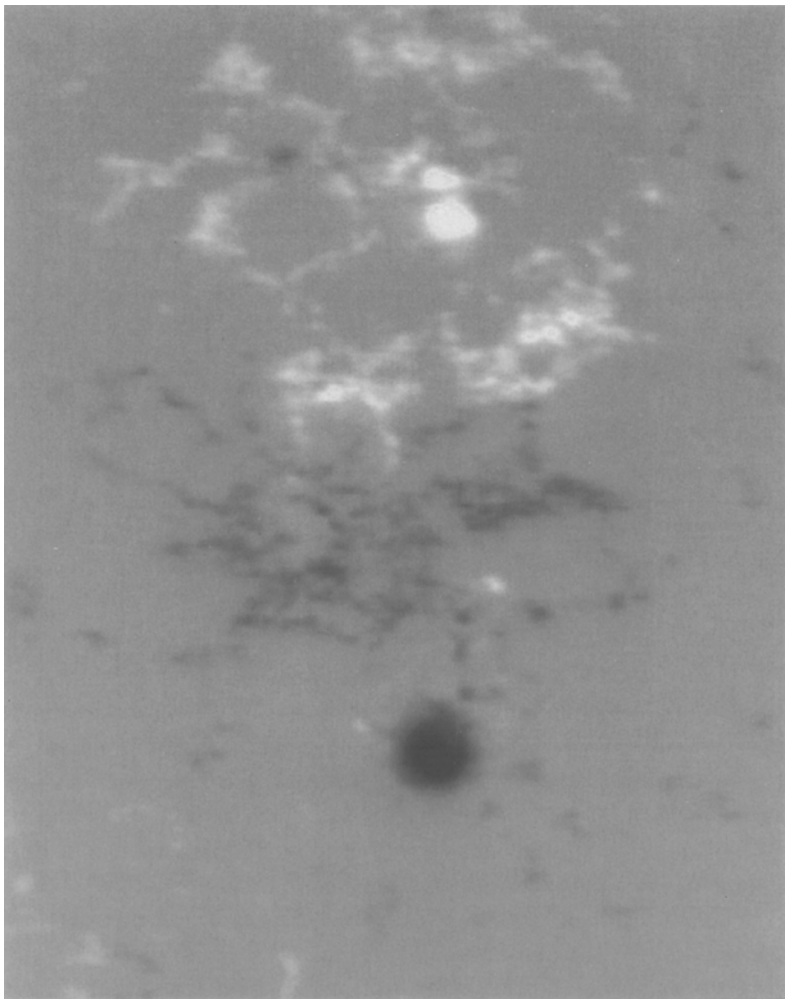

Fig. 2b.

Fig. 2a–b. Two images of NOAA AR 7558 from (a) the BBSO videomagnetograph and (b) the NASA/NSO spectromagnetograph, both taken on 6 August, 1993. The image from the NASA/NSO instrument is a small portion of the full-resolution daily full-disk image magnified to match the BBSO image scale. The BBSO image has been rotated so that heliographic north is at the top and east is at the left, to match the NASA/NSO image. Note that the light level in the sunspot umbra is too low in this case for the BBSO instrument to measure the magnetic field. However, the resolution of the BBSO image (selected from that day's magnetogram movie) is greater than the NASA/NSO image. In both images corresponding gray levels are at the same field strength.

In both cases the calibration is based on the weak-field approximation; that is, that the line profile $H(a,\, v \pm v_b)$ is approximated by the low-order terms of the Taylor series $H(a,\, v) \pm v_b H'(a,\, v) + (v_b^2/2)H''(a,\, v) + \cdots$, where H is a Voigt

function, a is inversely proportional to the Doppler width, and $V_b = \Delta\lambda_B/\Delta\lambda_D$ (Jefferies, Lites, and Skumanich, 1989).

Jefferies and Mickey (1990) showed that the weak-field approximation can be used for a much larger range of magnetic field strengths than previously thought, with v_b on the order of 1, if $\lambda_{\text{off}} > 2\Delta\lambda_D$. This gives the simple calibration schemes described here greater validity than was previously thought by some researchers. Another example of the application of the weak-field approximation to the calibration of a magnetograph is given by Rust and O'Byrne (1990).

2.1. SBP MODE CALIBRATION (PROFILE SLOPE METHOD)

For the longitudinal field, the basic relation is given by

$$V_{\text{diff}} = -\mu_\lambda B \frac{\mathrm{d}I}{\mathrm{d}\lambda}\,, \tag{2}$$

where V_{diff} is the V value obtained by subtracting one pair of frames taken in alternating KDP polarities *without* dividing by I and

$$\mu_\lambda = \frac{e\lambda^2 g}{4\pi m c^2}\,, \tag{3}$$

the magnetic moment of the transition. Here m and e are the mass and charge of the electron, λ is the wavelength of the transition, and g is the Landé factor expressing the departure from the normal Zeeman effect for this transition.

As a first approximation to the actual response of the system, the actual measured difference between two VMG frames of opposite KDP polarities can be designated V_{obs} such that $V_{\text{diff}} = \phi V_{\text{obs}}$, where ϕ is a measure of the response of the system. Similarly, when a frame is grabbed with the KDP off, one obtains I_{obs} where $I = \phi I_{\text{obs}}$.

Now what exactly do we mean by the response of the system? The actual measured value of V will include the response of the filter, and is given by

$$V_{\text{obs}} = P * V\,, \tag{4}$$

where P is the filter passband. This convolution was done for a system similar to ours by Rust and O'Byrne (1991). Their Equation (5) is reproduced below:

$$V_{\text{measured}} = P * V = \mu_\lambda B \cos\gamma \int P(\lambda - \lambda') \left(\frac{\mathrm{d}I}{\mathrm{d}\lambda'}\right) \mathrm{d}\lambda'\,, \tag{5}$$

where $B\cos\gamma$ is the longitudinal field.

Rust and O'Byrne (1991) show by modeling the convolution of their filter bandpass and a theoretical V profile that for an appropriate choice of the wavelength offset, the theoretical response of their system to magnetic field signals from the

Sun is linear. As is shown in Figure 5 below, the actual response of the Big Bear videomagnetograph, as compared to actual Zeeman splittings, is generally linear. This makes it reasonable to assume that the effect of the convolution of the V signal with the filter profile at the wavelength offset actually used in the Big Bear videormagnetograph can be included in the response parameter ϕ and can be considered constant for reasonable magnetic field values. It can be shown that the value of ϕ for I_{obs} is the same as that for V_{obs}, assuming that the magnetograph response is linear.

Here $\mathrm{d}I/\mathrm{d}\lambda$ is of course the slope of the line profile. Another way of expressing the basic idea of the weak field approximation is to say that the slope of the line profile is considered a constant independent of the Zeeman splitting.

Essentially the problem of calibrating the magnetograph becomes the problem of measuring this slope, using the magnetograph instrument. The slope is measured by adjusting the filter through a series of known wavelength offsets from the center of the line and grabbing frames at each wavelength offset. This allows the measured slope $\mathrm{d}I_{\text{obs}}/\mathrm{d}\lambda$ to be determined. Using the Big Bear videomagnetograph there is a range of wavelength offsets between about -40 mÅ and about -160 mÅ from the center of the 6103 Å line where the slope of the line profile is nearly constant.

Notice that ϕ will change not only as changes are made to the VMG system (e.g., changing neutral density filters or the gain of the A/D converter), but also throughout the day as the Sun's altitude changes. The calibration also effectively changes as the system is used to measure fields on different parts of the Sun (both due to limb darkening and to sunspots) because the video level of the continuum changes, thus changing the measured value of $\mathrm{d}I_{\text{obs}}/\mathrm{d}\lambda$. Thus if the VMG system operates (as the old Quantex system does) by only storing $\frac{1}{2}nV_{\text{obs}}$ (where n is the number of video frames in the magnetogram), the apparent field measured changes with the observed brightness of the Sun. In order to stabilize the measurements, one needs to store a quantity proportional to $V_{\text{obs}}/I_{\text{obs}}$. This is the second major difference between the Quantex and Datacube VMG systems, the first being the greater dynamic range of the 16-bit Datacube system. Images of this type (proportional to $V_{\text{obs}}/I_{\text{obs}}$) can be calibrated in the following way.

The Big Bear magnetograph operates by switching the KDP crystal between $+\frac{1}{4}$-wave and $-\frac{1}{4}$-wave states, thus switching between detecting right- and left-circular polarization. When transverse magnetic fields are to be measured the filterwheel is rotated to insert an appropriately-oriented $\frac{1}{4}$-wave plate to convert the linear-polarized light from the Sun to circular polarization. For longitudinal fields, if the Stokes vector of the incoming sunlight is $(IQUV)$ then for one polarity of the KDP the output intensity is $\frac{1}{2}(I_{\text{obs}} + V_{\text{obs}})$ and for the other it is $\frac{1}{2}(I_{\text{obs}} - V_{\text{obs}})$. Here it is assumed the KDP acts as a perfect $\frac{1}{4}$-wave plate and the first polarizer in the Zeiss filter also acts perfectly. The VMG system works essentially by storing in one 16-bit buffer in the Datacube the quantity

$$\frac{n}{2}\left(\frac{1}{2}(I_{\rm obs}+V_{\rm obs})\right)-\frac{n}{2}\left(\frac{1}{2}(I_{\rm obs}-V_{\rm obs})\right)\,, \tag{6}$$

which is equal to $\frac{1}{2}nV_{\rm obs}$, and in the other buffer the quantity

$$\left[\frac{n}{2}\left(\frac{1}{2}(I_{\rm obs}+V_{\rm obs})\right)+\frac{n}{2}\left(\frac{1}{2}(I_{\rm obs}-V_{\rm obs})\right)\right]\frac{1}{n}\,, \tag{7}$$

which is equal to $\frac{1}{2}I_{\rm obs}$. The contents of the Datacube buffers are then transferred to the VAX computer system and manipulated to yield (in 16-bit, calibrated mode) the value

$$V_{\rm sto}=\frac{256nV_{\rm obs}}{I_{\rm obs}}\,, \tag{8}$$

which is stored as a 16-bit integer FITS image. Here n is the number of video frames in the magnetogram. The factor of 256 is included so that precision is not lost when the integer division is done, and so that the result can be stored as a 16-bit integer rather than a 32-bit real number.

Then one can say:

$$\phi\frac{256nV_{\rm obs}}{I_{\rm obs}}=\frac{-256n}{I_{\rm obs}}\mu_\lambda B\frac{{\rm d}I}{{\rm d}\lambda}\,. \tag{9}$$

But ${\rm d}I/{\rm d}\lambda$ cannot be measured directly with the magnetograph. The magnetograph only measures ${\rm d}I_{\rm obs}/{\rm d}\lambda$, and ${\rm d}I/{\rm d}\lambda=\phi\,{\rm d}I_{\rm obs}/{\rm d}\lambda$. So,

$$\phi\frac{256nV_{\rm obs}}{I_{\rm obs}}=\frac{-256n}{I_{\rm obs}}\mu_\lambda B\phi\frac{{\rm d}I_{\rm obs}}{{\rm d}\lambda}\,. \tag{10}$$

Or,

$$V_{\rm sto}=\frac{-256n}{I_{\rm obs}}\mu_\lambda B\frac{{\rm d}I_{\rm obs}}{{\rm d}\lambda}\,. \tag{11}$$

Then

$$B=\frac{-V_{\rm sto}}{256n}\left[\frac{1}{\mu_\lambda}\frac{{\rm d}\lambda}{{\rm d}I_{\rm obs}}I_{\rm obs}\right]\,. \tag{12}$$

Notice that

$$\frac{{\rm d}\lambda}{{\rm d}I_{\rm obs}}I_{\rm obs}=\frac{\phi\,{\rm d}\lambda}{{\rm d}I}\frac{I}{\phi}=\frac{{\rm d}\lambda}{{\rm d}I}I\,, \tag{13}$$

so this quantity does not have to be measured at the same time as $V_{\rm sto}$. If the constant k_1 is defined such that

$$k_1 = \left[\frac{-1}{\mu_\lambda}\frac{\mathrm{d}\lambda}{\mathrm{d}I}I\right] , \tag{14}$$

then

$$B = k_1\frac{V_{\mathrm{sto}}}{256n} . \tag{15}$$

This result can be compared with that from the Doppler calibration obtained below. A similar result could be obtained for the transverse field, which would however depend explicitly on the wavelength offset of the filter from the center of the line. It could be argued, however, that the passband of the Zeiss filter is too wide for such a formula to be valid for transverse fields. Therefore I will use an empirical transverse field calibration (see Section 3.3 below).

Typically the line profile is measured by averaging over an entire image and thus refers mainly to the quiet Sun. Some measurements of penumbral areas have been made, however, and they will be discussed below. The slope of the line profile is measured by taking intensity images, adjusting the position of the Zeiss filter passband by 18 mÅ each time. The center of the line is found, and the slope is obtained by taking the average intensity at each position between about -40 mÅ from the line center and about -160 mÅ from the line center, or as far out from the line as the profile was measured. In this wavelength range the line profile (convolved with the Zeiss filter passband) is roughly linear. The range brackets our standard single bandpass offset of -110 mÅ.

2.2. DBP MODE CALIBRATION (DOPPLERGRAM METHOD)

The calibration of the double bandpass mode (Ramsey, 1971) is also based on the weak field approximation. The shift produced by a known Doppler shift (due to solar rotation) produces a change in the difference signal of the magnetograph when a circular polarizer is introduced into the beam. The signal produced by this known wavelength shift is affected by the measured slope of the line profile $\mathrm{d}I/\mathrm{d}\lambda$ just as the magnetic field signal is, and can be compared to signals produced by the wavelength shifts generated by solar magnetic fields. The Landé g-factor of the Ca I line is 2.0. As shown in Shi, Wang, and Patterson (1986), for a magnetic field of 1000 G, the wavelength shift is 0.03479 Å. In other words, a Doppler signal of 1 km s^{-1} corresponds to a field of 584.7 G.

The magnetograph in double bandpass mode can be thought of as two single bandpass magnetographs on opposite sides of the center of the line, where the displacement of the two passbands is determined by the construction of the Zeiss filter. One side gives a positive difference signal for right circularly polarized light while the other side gives a positive signal for left circularly polarized light. Since the Zeeman effect leads to opposite polarizations on either side of the line from a given magnetic feature, the signals from the two parallel systems add together. The signal stored by the magnetograph is

$$V_{\rm sto} = \frac{256n(V_{\rm obs1} + V_{\rm obs2})}{(\langle V_{\rm obs1}\rangle + \langle I_{\rm obs2}\rangle)}\,, \tag{16}$$

where $V_{\rm obs1}$ is the difference between two video frames in one passband, $I_{\rm obs1}$ is the intensity from a single frame in the same passband, and $V_{\rm obs2}$ and $I_{\rm obs2}$ refer to the other passband.

In Doppler mode, all of the incoming light is made right circular polarized by a circular polarizer. The signal stored by the magnetograph is the same as for a DBP magnetogram. In one KDP orientation only the light from the blue side of the line is recorded, in the other only the light from the red side is recorded. Therefore when n frames are recorded in the Datacube the difference buffer will contain

$$\frac{n}{2}(I_V - I_R)$$

and the average buffer will contain

$$\frac{n}{2}(I_V + I_R)\frac{1}{n}\,.$$

To first order,

$$I_R = I_0 - \frac{{\rm d}I}{{\rm d}\lambda}\frac{v}{c}\lambda \quad \text{and} \quad I_V = I_0 + \frac{{\rm d}I}{{\rm d}\lambda}\frac{v}{c}\lambda\,,$$

where I_0 is the intensity in the passband of an unshifted area on the Sun. Then the stored Doppler image is

$$D_{\rm sto} = \frac{256}{I_0}\frac{n}{2}\frac{2\,{\rm d}I}{{\rm d}\lambda}\frac{\lambda}{c}v\,. \tag{17}$$

So,

$$v = \frac{D_{\rm sto}}{256n}\left[\frac{c}{\lambda}I\frac{{\rm d}\lambda}{{\rm d}I}\right]\,. \tag{18}$$

It is easy to see by analogy with the single bandpass calibration that the quantity in the brackets is a constant. This quantity can be found empirically by dividing the Dopplergram signal by the velocity. However, the effective slope of the profile here is not going to be the same as for the SBP magnetogram because the offset from line center is fixed by the construction of the filter. To allow for different integration lengths when calibrating, $V_{\rm sto}$ is divided by $256n$, where n is the number of frames in the VMG. The magnetic field is then given by

$$B = C\frac{V_{\rm sto}}{256n}\,, \tag{19}$$

where

TABLE I

Doppler and line profile calibration results for the first half of 1993

Date	Doppler			Line profile (k_1)	
	C (average)	f	Cf	Quiet Sun	Penumbra
21 Jan., 1993	19835	0.66	13100		
27 Jan., 1993	20491	0.717	14700	13770	
25 Feb., 1993	19867	0.725	14400	10740	16900
4 March, 1993				10620	12090
2 Apr., 1993	17130	0.725	12400		
28 Apr., 1993				11980	
5 May, 1993				11150	
10 May, 1993				10620	
28 May, 1993	17927	0.734	13200		
Average	19050	0.712	13600	11480	14500

$$C = \frac{584.7v}{\langle D_{\text{sto}} \rangle / (256 n_D)} , \tag{20}$$

v is the average solar rotation velocity in km s^{-1} for the Doppler image, and n_D is the number of frames in the Doppler image.

In order to avoid the effects of the velocity fields in active regions, only quiet Sun areas are used to obtain the Dopplergrams. Typically, images are obtained at three positions: heliographic disk center (N 0° W 0°) and at N 0° E 20° and N 0° W 20°. The filter is first tuned so that the average signal at disk center is zero. Then Doppler images are obtained at each position, typically using an integration length of 128 frames. The relative change in velocity between the images then only depends on the solar rotation, a known quantity. When calibrated observations in DBP mode are desired, the filter is tuned so that the average Doppler signal is zero. Since active regions have velocity features of their own, either quiet Sun areas at the edge of the image or a quiet Sun area at opposite heliographic latitude is used to determine the velocity zero point.

To apply the Doppler calibration to single bandpass mode magnetograms, magnetograms of the same region are taken in both modes and the factor $f = V_{\text{sto DBP}}/V_{\text{sto SBP}}$ is obtained. This factor is tabulated in Table I for the period January to May 1993. The average value was found to be 0.71. Then for single bandpass mode

$$B = Cf \frac{V_{\text{sto}}}{256n} . \tag{21}$$

It should be noted that this method of finding f will weight the penumbra of active regions most strongly, since that is the area where the magnetograph signals

are strongest in both single and double bandpass modes. The reason for this is that the magnetic flux in the penumbra is high and the intensity is high as well (relative to the umbra), thus the difference between video frames taken in alternating KDP polarities will be large. In the quiet Sun, the magnetic flux is low, thus producing a low magnetograph signal. In sunspot umbrae, the flux is high but the light level is low, producing a small difference signal. Even though the magnetograph divides the difference by the intensity to produce V_{sto}, if the difference is small it will be lost in the noise before the division can be done.

2.3. CALIBRATION USING SPECTRA

The simplest way of detecting magnetic fields on the Sun is, of course, to measure directly the splitting of a Zeeman-sensitive line in a spectrogram as was originally done by Hale in 1908 (Hale and Nicholson, 1938). An obvious way to calibrate the magnetograph, then, is to measure simultaneously the field in a sunspot using both a spectrograph and the magnetograph. Then the splitting observed in the spectrogram can be used to calibrate the signal observed in the magnetogram.

The Zeeman splitting measures the total magnetic field, and cannot be compared directly to a longitudinal magnetogram in situations where the magnetic field is not expected to be substantially vertical, as in the penumbra of a sunspot. However, this does provide the opportunity to use the spectral splitting as an aid in calibrating transverse field measurements.

However, the Zeeman splitting cannot simply be measured in the line used by the magnetograph because the magnetograph operates on the basis of the weak-field approximation. This requires, essentially, that the spectral splitting caused by the magnetic field not be resolved by the filter system used in the magnetograph. Simply speaking, it is the resolution of the splitting by the magnetograph system that causes 'saturation' of the magnetogram signal (the nonlinear response of the magnetograph to strong fields). The line used for the magnetograph must be chosen so that this saturation does not occur for field strengths of interest. As is shown below, this is the case for the 6103 Å line and the Big Bear Zeiss filter. On the other hand, a large amount of splitting is needed to resolve the Zeeman components in the spectrum. Therefore, the splitting should be measured in a line with a higher Landé g-factor than the one being used by the magnetograph and it must be assumed that the magnetic field shown by the Zeeman splitting is the same as that measured by the magnetograph. Further, it is assumed that the response of the magnetograph at field strengths below the point where the Zeeman splitting can be measured in the spectrogram is linear.

Any magnetograph can only really measure magnetic flux. Therefore the effect of seeing on a magnetogram will be in general to reduce the measured field strengths, as the effective resolution element size of the magnetograph is increased. On the other hand, seeing will not reduce the amount of splitting observed in a spectrograph as long as any splitting can be detected. By calibrating in a spot penumbra,

where the magnetic field is fairly uniform, the effect of seeing can be reduced or eliminated. Since the line splitting depends on the magnetic field strength, and not the magnetic flux, the field measured by the spectrograph is independent of seeing (again, so long as the splitting can be detected).

Here I will use the Fe I 5250 Å line for the spectrum, and the Ca I 6103 Å line for the magnetogram. The Fe I 5250 Å line, with a Landé g-factor of 3, is somewhat more sensitive to magnetic fields than the Ca I 6103 Å line, which has a Landé g-factor of 2. In general, one would expect a high degree of correlation between the magnetic field strengths measured in different photospheric lines. This can be seen, for example, in the correlation between the BBSO and NASA/NSO magnetograms shown in Figure 2. Here the BBSO magnetogram is in the Ca I line while the NASA/NSO magnetogram uses the Fe I 8688.6 Å line. One could expect a systematic difference to be seen, however, depending on the differing heights of formation for each line. These two lines are of similar strengths, with the Ca I line somewhat stronger. The ionization energies are not very different from each other. Intuitively one would expect the Ca I line to form at a somewhat greater height in the atmosphere. Grossmann-Doerth (1994) shows that the height of formation of a photospheric line is also affected by the excitation energy of the lower atomic state of the transition. The lower value for the excitation energy of the lower atomic state in the Fe I line (0.12 eV as compared to 1.87 eV for Ca I) suggests that the upper end of the formation depth range for the Fe I line is higher than what would be otherwise expected based only on the line strengths. In addition, any systematic difference seen in the magnetic field would also depend on the dependence of the field with height in the photosphere. In fact, the height of formation of a spectral line itself depends on the degree of Zeeman splitting (see, for example, Larsson, Solanki, and Grossmann-Doerth, 1991). For the purposes of this paper I will assume that the difference in the height of formation of these lines can be neglected.

In order to have sufficient signal in the magnetogram (in the spot umbra the intensity of the input video frames is very low, thus the signal-to-noise ratio in the magnetogram is poor), the magnetogram and spectrogram must be compared in the penumbra of a sunspot. In the spot penumbra, the transverse fields are stronger than the longitudinal fields, and therefore the total field value obtained by the magnetograph depends mainly on the transverse magnetograms. Thus the Zeeman splitting provides a useful way to calibrate transverse magnetograms.

3. Discussion

3.1. The Doppler calibration

Figure 3 shows the values of C for each set of calibration measurements from January 1991 to May 1993. The data show that over short periods (weeks), the Doppler calibration remains stable to within about 20%, agreeing with the result

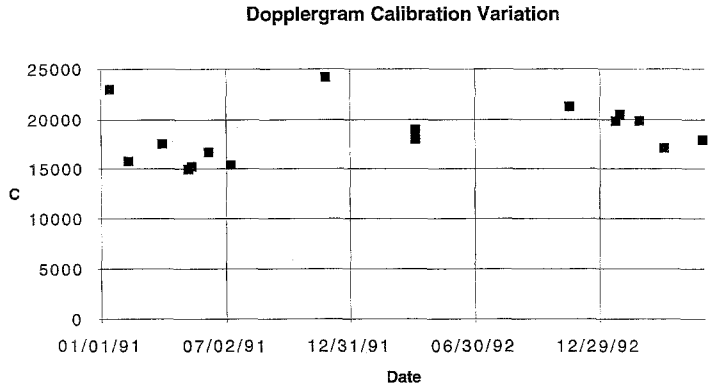

Fig. 3. Variation of the double bandpass calibration parameter C as a function of time from January 1991 to May 1993.

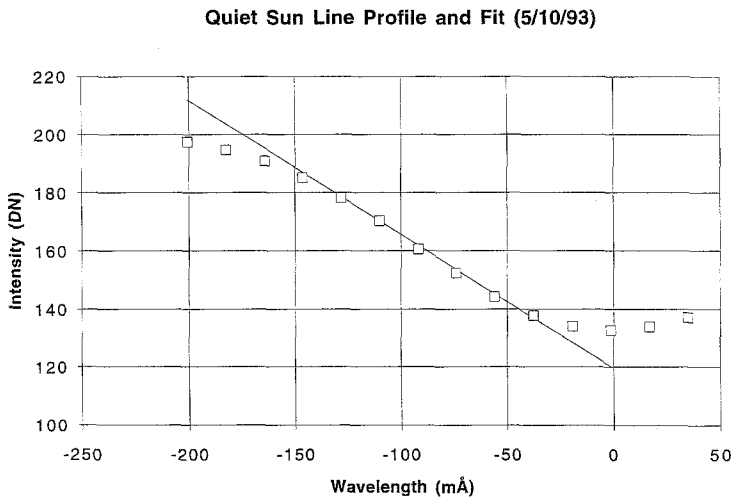

Fig. 4. Line profile measured in quiet Sun at 6103 Å on 10 May, 1993. The linear fit used to determine $dI/d\lambda$ is also shown. The offset used for the single bandpass magnetograms is -110 mÅ. For magnetic fields of 2100 G or less, corresponding to line shifts of 70 mÅ or less, the observed line profile does not depart significantly from linearity, thus saturation does not occur.

of Shi, Wang, and Patterson (1986). Over longer time scales, larger variations are observed. It is possible that these are due to temperature variations in the KDP crystal. In the winter months, the temperature of the system is systematically lower than in the summer, which decreases the sensitivity as the KDP crystal is not acting precisely as a $\frac{1}{4}$-wave plate. This appears to be true even though the system is enclosed by the foam-core box.

It is also gratifying to see that there is no systematic difference in the calibration before and after the 1992 June 28 earthquake, which stopped observations for four

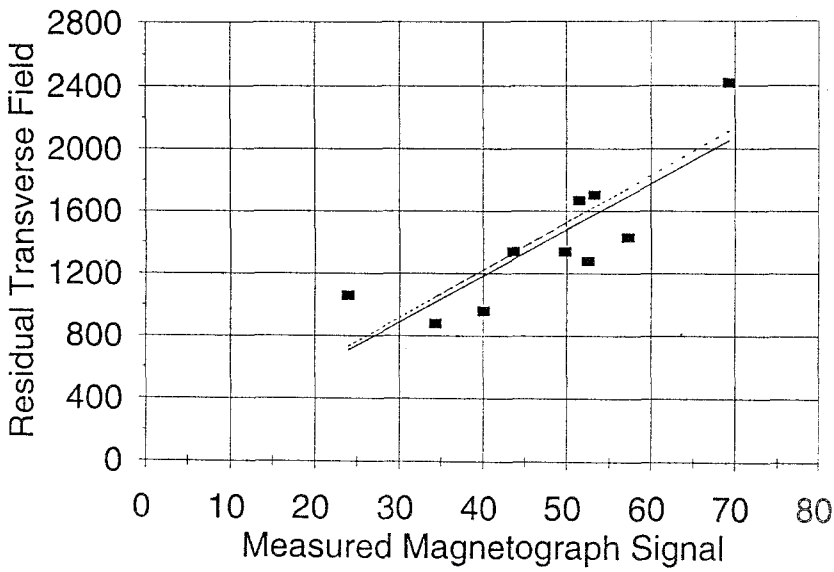

Fig. 5. Comparison of the residual transverse field (obtained by subtracting in quadrature the longitudinal magnetic field from the magnetograph at 6103 Å from the total magnetic field values from Zeeman splitting in 5250 Å spectra) with the signal from the Big Bear videomagnetograph in transverse field mode. The solid line is a linear fit to the data shown. The dashed line is the relationship between magnetograph signal and transverse field obtained from a formula based on the slope of the 6103 Å line profile. The data are from NOAA AR 7440 obtained on 8 March, 1993.

months while the telescope was disassembled, the pier partially replaced, and the telescope reassembled.

3.2. THE LINE PROFILE METHOD AND COMPARISON WITH DOPPLER CALIBRATION

Calibration measurements made between 27 January, 1993 and 28 May, 1993 are listed in Table I and shown in Figure 8. Measurements using both the Dopplergram method (the values for C, f, and Cf) and the line profile method (the values for k_1) are shown. The line profiles were measured mainly for quiet Sun, but also for penumbrae for two dates. The wavelength offset for SBP mode was 110 mÅ in all cases. A typical line profile for the quiet Sun is shown in Figure 4 along with the linear fit to the line profile. So long as the intensity measured in the Zeeman-shifted line does not depart significantly from the linear fit, the magnetograph calibration should be valid. In this case, saturation of the magnetograph should not occur below $\Delta\lambda_H$ of 70 mÅ, or a magnetic field strength of at least 2100 G.

The longitudinal magnetic field calibration parameter (Cf) values obtained using the Dopplergram calibration are on average 18% higher than those using the quiet-Sun line profile calibration (k_1). However, if the Dopplergram calibrations are compared to the average penumbral line profile calibration, it turns out that the

(a)

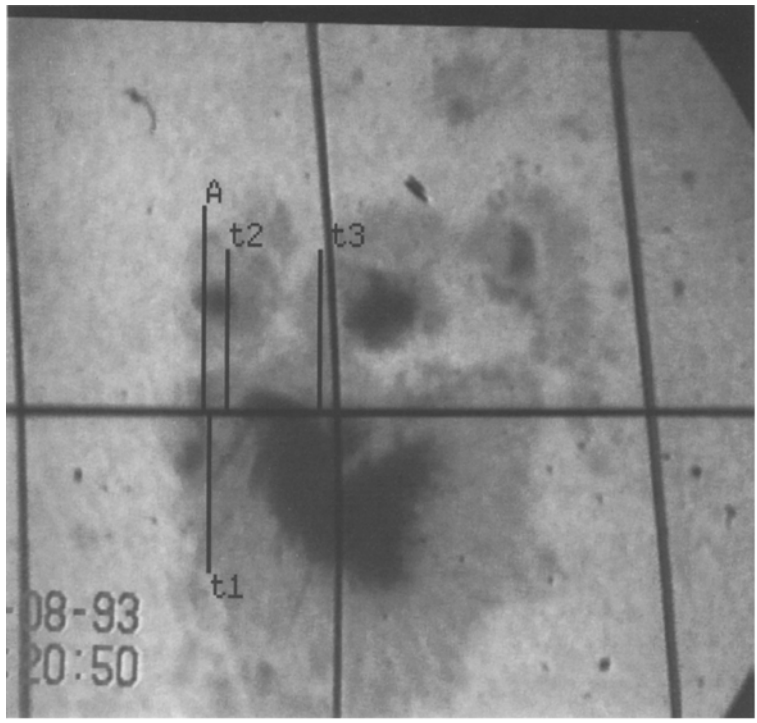

(b)

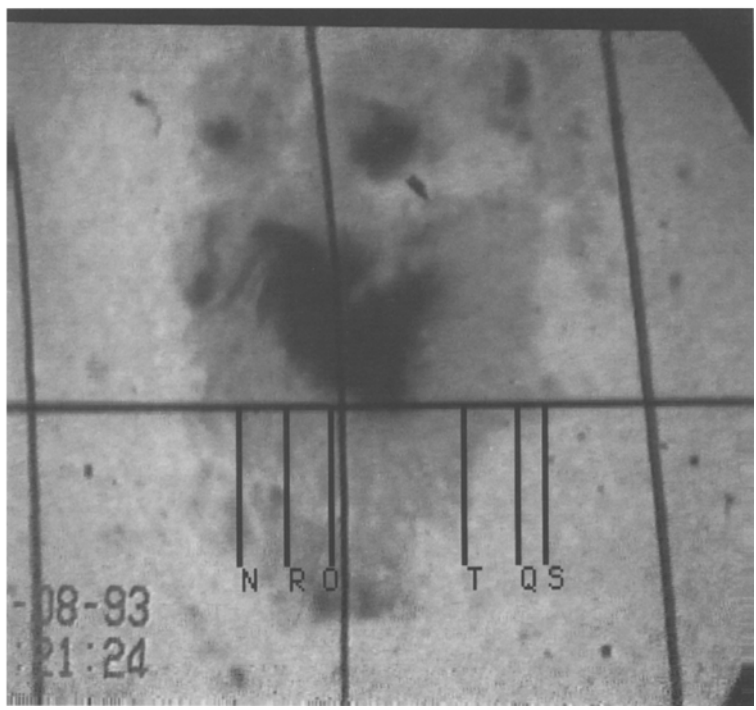

Fig. 6. White-light Big Bear spectrograph slit-jaw images showing positions measured in Zeeman spectra and magnetograms for comparison of derived magnetic field values on 8 March, 1993. The region is NOAA AR 7440.

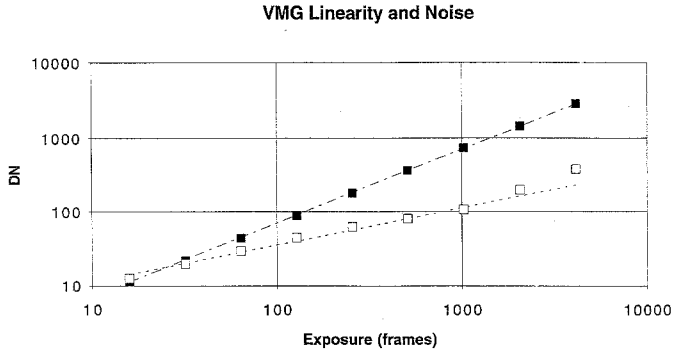

Fig. 7. Videomagnetograph signal and noise levels as a function of the number of video frames in the exposure. Based on enhanced network images obtained in single bandpass mode on 18 November, 1992. The signal is indicated by filled squares, the noise by open squares.

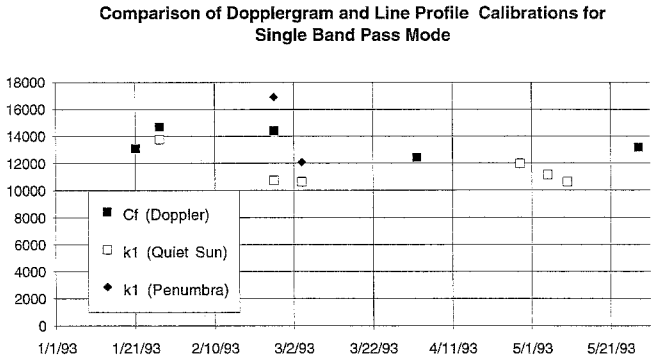

Fig. 8. Comparison of single bandpass calibration parameters from January to May 1993. Filled squares are Cf values from the Doppler calibration technique. Open squares are k_1 values from quiet-Sun line profiles. Filled diamonds are k_1 values from penumbral line profiles.

Dopplergram calibration Cf value is 6% lower than the penumbral line profile k_1 value. This is reasonable if one considers that C, f, and k_1 will all depend on the shape of the solar line profile as well as the filter passband. The Doppler calibration constant, C, is always obtained from quiet-Sun areas, while the double to single bandpass factor f is obtained from active regions. Therefore it is reasonable that Cf should lie between k_1 obtained from the quiet Sun and k_1 obtained from penumbrae. We plan to obtain values of f from quiet-Sun areas for comparison with the current penumbral f values.

3.3. Comparison with Zeeman Spectra

Simultaneous magnetograms and spectrograms were obtained on 8 March, 1993 using the spectrograph on the 65-cm telescope and the videomagnetograph in single bandpass mode on the 25-cm telescope of Big Bear Solar Observatory. The

TABLE II

Comparison of magnetic fields obtained from spectrum and magnetogram on 8 March, 1993. All fields measured in gauss. The average K_1 value for the penumbra were used in the calibration of the magnetograms. The last column is the signal from the magnetograph operated in transverse field mode, in arbitrary units.

Position	Spectrum total field B	Longitudinal field B_L	Residual trans. field B_T	Magnetograph trans. signal $(Q_{\text{sto}}^2 + U_{\text{sto}}^2)^{1/4}$
t_1	1860	819	1670	51.5
t_2	2430	266	2420	69.3
t_3	1200	561	1060	24.0
A	1600	714	1430	57.2
R	1400	555	1280	52.5
S	900	194	880	34.4
T	1480	632	1340	49.8
O	1955	732	1704	53.3
N	1420	455	1340	43.7
Q	1030	363	960	40.1

observations were made of NOAA AR 7440. This region had a prominent magnetic polarity inversion line, offering the possibility of strong organized penumbral transverse fields. Figure 6 shows the locations of the measurements in the spectrograph slit-jaw images. The longitudinal magnetograms were obtained using 128 video frames, while measurements taken in transverse mode (measurements of Q and U) were also obtained using 256 video frames each.

Table II lists the values of the total field measured by the splitting, the longitudinal field measured by the magnetograph using the average value of k_1 found for penumbrae, as well as the value of the transverse field given by $(B_T^2 - B_L^2)^{1/2}$, where B_T is the total field from the Zeeman splitting and B_L is the longitudinal field from the magnetogram. Also listed is the measured quantity $(Q_{\text{sto}}^2 + U_{\text{sto}}^2)^{1/4}$, where Q_{sto} and U_{sto} are measured using the magnetograph in the configuration described in Section 1. This quantity should be proportional to the transverse field, provided that the field is not so large as to cause splitting that is greater than the linear part of the spectral line profile, when convolved with the filter passband, and that the quantities Q_{sto} and U_{sto} are proportional to the actual linear polarization of the incoming sunlight.

The results of a comparison between the residual transverse field as determined by combining the total field measured by the Zeeman spectra and the longitudinal field measured by the magnetograph and the measured quantity $(Q_{\text{sto}}^2 + U_{\text{sto}}^2)^{1/4}$ is shown in Figure 5. The solid line represents a linear fit, while the dashed line indi-

cates the relationship between the signal measured by the transverse magnetograph and the transverse magnetic field that would be obtained using a formula similar to the one developed for the longitudinal field in Section 2.1. There appears to be no significant difference between the empirical fit and a transverse field calibration based on the slope of the line profile. Therefore, from the measurements made so far, it appears that one could use such a calibration with the Big Bear instrument.

The calibration empirically obtained using the Zeeman spectra is then (based on the linear fit)

$$B_T = 29.75(Q_{\text{sto}}^2 + U_{\text{sto}}^2)^{1/4} - 7.2\,, \tag{22}$$

remembering that there are 256 video frames in each Q and U measurement. If it is permitted to generalize for different integration lengths, one obtains

$$B_T = \frac{476}{n^{1/2}}(Q_{\text{sto}}^2 + U_{\text{sto}}^2)^{1/4} - 7.2\,. \tag{23}$$

3.4. Linearity and Noise

In spite of the large number of elements affecting the linearity and noise characteristics of the BBSO Datacube VMG system, the system behaves very much as a linear device with the noise dominated by photon statistics. Figure 7 shows videomagnetograph signal and noise levels as a function of exposure time for an area of enhanced network. Pairs of magnetograms from 16 to 4096 frames in length were obtained in single bandpass mode on 1992 Novermber 18. The noise was estimated by subtracting one member of each pair from the other. The noise increases as the square root of the signal for short- and intermediate-length exposure times, as would be expected for photon noise. The dark current is insignificant. For very long exposures (longer than 1024 frames) the noise increases faster than the square root of the signal, suggesting that other factors, such as image motion during the exposure, are affecting the results for such long exposures.

4. Conclusions

The magnetograph calibration methods discussed here are reasonably consistent with each other and with the spectra, especially if the penumbral line profile is used for the single bandpass mode. The comparison with the spectra is based on a limited amount of data, but I expect that improvements in the BBSO spectrograph (especially the use of a high-resolution CCD camera in place of the current video camera) will allow the Zeeman splittings of weaker fields to be measured.

The calibrations discussed here apply only to magnetograms obtained on the 25-cm Big Bear telescope using the Datacube image processor and the 6103 Å

filter. Calibration parameters for other telescope and filter combinations will be forthcoming.

Currently magnetograms can be obtained over the Internet by interested researchers by using anonymous FTP to *suncub.bbso.caltech.edu*. The images in our public-access archive are scaled to 8 bits to save space and display particular magnetic features; for current images, calibrated pixel values (based on previous calibrations) can be obtained by scaling the pixels using the FITS header parameters BZERO and BSCALE. Since the calibration values do change with time, these values of BZERO and BSCALE should be considered preliminary. To obtain the best calibration parameters for particular images, contact BBSO. Older images in the archive do not have calibrated BZERO and BSCALE values; to obtain instructions for calibration as well as copies of the original 16-bit images, contact BBSO.

Acknowledgements

I am grateful to H. Zirin for discussions concerning the analysis of the spectra in this work, as well as the other observers at Big Bear Solar Observatory for helping to obtain the data. I am also grateful to Glenn Eychaner for producing the current much improved and highly efficient version of the magnetograph software.

This work was supported by ONR grant number N00014–89-J-1069, NSF grant number ATM-9122023, and NASA grant number NAGW-1972.

References

Babcock, H. D. and Babcock, H. W.: 1952, in G. Kuiper (ed.), *The Sun*, University of Chicago Press, Chicago, Ill., p. 704.

Cacciani, A., Varsik, J., and Zirin, H.: 1989, *Solar Phys.* **125**, 173.

Grossmann-Doerth, U.: 1994, *Astron. Astrophys.* **285**, 1012.

Hale, G. E. and Nicholson, S. B.: 1938, *Magnetic Observations of Sunspots, 1917–1924, Part I*, Publ. Carnegie Inst. No. 498.

Jefferies, J. T. and Mickey, D. L.: 1991, in L. J. November (ed.), *Solar Polarimetry*, National Solar Observatory, Sunspot, N.M., p. 373.

Jefferies, J. T., Lites, B. W., and Skumanich, A.: 1989, *Astrophys. J.* **343**, 920.

Larsson, B., Solanki, S. K., and Grossmann-Doerth, U.: 1991, in L. J. November (ed.), *Solar Polarimetry*, National Solar Observatory, Sunspot, N.M., p. 479.

Leighton, R. B.: 1959, *Astrophys. J.* **130**, 366.

Mosher, J. M.: 1976, 'The Caltech Videomagnetograph', BBSO Preprint No. 0159.

Ramsey, H. E.: 1971, *Solar Phys.* **21**, 54.

Rust, D. M. and O'Byrne, J. W.: 1991, in L. J. November (ed.), *Solar Polarimetry*, National Solar Observatory, Sunspot, N.M., p. 74.

Shi, Z., Wang, J., and Patterson, A.: 1986, 'The Calibration of Dopplergrams and Magnetograms at BBSO', BBSO Preprint No. 0257.

Smithson, R. C.: 1972, Thesis, Caltech.

Smithson, R. C. and Leighton, R. B.: 1971, in R. Howard (ed.), 'Solar Magnetic Fields', *IAU Symp.* **43**, 76.

Shurcliff, W. A.: 1962: *Polarized Light*, Harvard University Press, Cambridge, Massachusetts.

Wang, H., Varsik, J., Zirin, H., Canfield, R., Leka, K. D., and Wang, J.: 1992, *Solar Phys.* **142**, 11.

Zirin, H.: 1986, *Australian J. Phys.* **38**, 961.